

Coupling Between Periodic and Aperiodic Variability in SAX J1808.4-3658

M. T. Menna

*Osservatorio Astronomico di Roma, via Frascati 33, I-00040 Monteporzio Catone (Roma),
Italy.*

menna@coma.mporzio.astro.it

L. Burderi

*Osservatorio Astronomico di Roma, via Frascati 33, I-00040 Monteporzio Catone (Roma),
Italy.*

L. Stella

*Osservatorio Astronomico di Roma, via Frascati 33, I-00040 Monteporzio Catone (Roma),
Italy.*

N. Robba

*Dipartimento di Scienze Fisiche ed Astronomiche, Università di Palermo, via Archirafi 36,
I-90123 Palermo, Italy.*

M. van der Klis

*Astronomical Institute Anton Pannekoek, University of Amsterdam, Kruislaan 403, 1098
SJ Amsterdam, The Netherlands*

ABSTRACT

We detect a significant broadening in the wings of the 401 Hz peak in the power spectrum of the accreting millisecond binary pulsar SAX J1808.4-3658. This feature is consistent with the convolution of the red noise present in the power spectrum with the harmonic line. We conclude that the flux modulated by the spin period shows aperiodic variability similar to the red noise in the overall flux, suggesting such variability also originates at the magnetic caps close to the neutron star surface. This is analogous to the results found in some longer period, higher magnetic field pulsators in high mass X-ray binaries.

Subject headings: pulsars: individual (SAX J1808.4-3658) — accretion — stars: magnetic fields — stars: neutron — X-rays: stars

1. Introduction

The power density spectra of low mass X-ray binaries show broad band noise components, produced by aperiodic variability, the sum of which typically rises towards lower frequencies (sometimes flattening below a frequency ν_{knee}) and is often termed red noise. Other power spectrum features are often present, including relatively broad peaks, quasi periodic oscillations, bumps, wiggles and low frequencies excesses (see *e.g.* Wijnands & van der Klis 1999 for a review). In many respects these noise components are similar to those observed in high mass X-ray binaries, containing X-ray pulsators and black hole candidates (see *e.g.* Belloni & Hasinger 1990). The continuum component of the red noise is usually modeled by broken power laws and/or Lorentzians.

In power spectra of X-ray pulsators a number of harmonic lines arising from the modulation of the flux due to the neutron star spin is also present. In this case, information on the regions giving rise to the aperiodic variability can be extracted from the study of the power spectra (Burderi *et al.*, 1997, hereafter B97; Lazzati and Stella, 1997, hereafter LS97). Indeed, if all or part of the aperiodic variability is produced by matter funneled by the magnetic field lines and accreting onto the magnetic polar caps of the neutron star, a modulation of that part of the aperiodic signal at the spin period would be expected (harmonic coupling). In the power spectra this would appear as a broadening of the wings of the harmonic lines due to the convolution of each harmonic line with the red noise (Burderi, Robba & Cusumano 1993) that produces a rescaled version of the red noise placed at both sides of each harmonic peak. Alternatively, if none of the aperiodic variability is generated in the funneled matter, the periodic and red noise features are expected to be independent of each other and there should be no broadening at the base of the harmonic lines.

A significant broadening in the wings of the harmonic lines was detected in the power spectra of some X-ray pulsators (B97; LS97), indicating that aperiodic variability is modulated at the spin period of the neutron star, *i.e.* produced at the neutron star magnetic polar caps. More recently, a coupling between the period and aperiodic variability of Hercules X-1 has been reported (Moon & Eikenberry 2001).

In 1998 the first millisecond accretion powered X-ray pulsar was discovered with the Rossi X-ray Timing Explorer (RXTE) by Wijnands & van der Klis (1998a). The pulsation frequency was ~ 401 Hz and showed a periodic modulation at 2.01 hours testifying to the presence of a low mass companion orbiting the neutron star with a mass function of the secondary star of $3.8 \times 10^{-5} M_{\odot}$ (Chakrabarty & Morgan 1998). The source was identified with SAX J1808.4-3658, a transient first detected with Beppo SAX in 1996 which displayed type I X-ray bursts and was classified as a low mass X-ray binary at an estimated distance of 4 kpc (in 't Zand *et al.* 1998). This distance has been recently updated to 2.5 kpc (in 't

Zand et al. 2001). The coherent pulsation was detected during the 1998 outburst when the source was repeatedly observed with RXTE from the 11th of April to the 6th of May. The source reached a peak luminosity of 3×10^{36} erg s⁻¹ on the 13th of April and then faded gradually below 10^{35} erg s⁻¹ by the 6th of May. Throughout this period the X-ray spectrum remained stable, featuring a power law shape with a photon index ~ 2 in the 15-100 keV band and a high energy cut-off above about 100 keV, similar to the X-ray spectra of other type I bursters in their low state (Gilfanov et al. 1998; Heindl & Smith 1998). Wijnands & van der Klis (1998b) studied the rapid aperiodic variability and revealed the presence of a red noise component in the power spectra flattening below a knee frequency $\nu_{knee} \sim 1$ Hz. The periodic modulation was nearly sinusoidal in shape and the power spectra displayed a very pronounced coherent peak at ~ 401 Hz.

The possibility of detecting a modulation at the spin frequency in the aperiodic variability depends crucially on the spin frequency: if this is too low, *i.e.* $\nu_{spin} \ll \nu_{knee}$ the broadening of the harmonic line’s wings is so wide that it blends in the red noise itself (B97; LS97). However, for SAX J1808.4-3658 $\nu_{spin} \gg \nu_{knee}$, which means that the typical duration of the aperiodic variations is many spin cycles, making this source a particularly well suited candidate to search for the presence of a coupling between this red noise component and the periodic variability.

2. The model

Analytic derivations of the power spectrum of a signal consisting of aperiodic variability, a periodic modulation and a coupling of the two was described by B97 and LS97. Our aim is to use an analytic function to fit the power spectrum of the SAX J1808.4-3658 to derive the entity (if present) of the coupling. In line with B97, we adopt randomly occurring shots as a convenient description of the aperiodic variability giving rise to the red noise (shot noise model). In this model the aperiodic variability is produced by a random superposition (in the light curve) of shots. These instabilities might originate in the accretion flow onto the compact object. We note that we can apply this model without loss of generality, as the coupling effect is independent of the mathematical model adopted to describe the red noise. In the following we briefly summarize some useful definitions and results from B97.

Our shot noise process $\mathcal{N}_{sn}(t)$ is obtained from the random superposition of identical shots occurring at a constant mean rate λ : the shot magnitude is $S = \int h(t)dt$, where $h(t)$ is the intensity profile of a shot. This means that the average intensity of the shot component is $\bar{I}_{sn} = \lambda S$. We indicate the power spectrum of the individual shot as $|H(\nu)|^2$.

A signal $I(t)$, as seen by a distant observer, emitted by a rotating neutron star of spin period P is, in general, composed by:

- a) a (constant) background component I_{bck} ;
- b) an emission (diffuse) arising from matter not funneled on the neutron star magnetic caps $I_{\text{DF}}(t)$ and therefore not affected by the periodic modulation induced by the neutron star rotation;
- c) a modulated (localized) component arising from matter accreting onto the magnetic poles $I_{\text{LC}}(t)$. The periodic modulation function $M(t)$, representing the geometric lighthouse effect produced by the neutron star rotation, is a series of identical pulse profiles of period $P = 1/\nu_0$. Expanded in Fourier series $M(t) = C + \sum_k c_k \cos(2\pi k \nu_0 t + \phi_k)$. In the case of SAX J1808.4-3658 the pulse profile is almost sinusoidal and we can approximate $M(t) \simeq C + c_1 \cos(2\pi \nu_0 t)$. We require $0 \leq M(t) \leq 1$, this poses a constraint on C and c_1 , namely, $C = 1 - c_1$. Thus we have

$$I(t) = I_{\text{bck}} + I_{\text{DF}}(t) + I_{\text{LC}}(t) \times M(t).$$

Let us assume that the diffuse and localized emission are each composed of a shot noise component and a constant component: we assume that the shot magnitude S and profile $h(t)$ is the same for both the shots arising in the localized and in the diffuse regions, while the shot rates are respectively λ_{LC} and λ_{DF} . K_{DF} and K_{LC} are respectively the constant emission of the diffuse and localized components of the signal. Thus we have:

$$I_{\text{DF}}(t) = K_{\text{DF}} + \mathcal{N}_{\text{sn}}(t)_{\text{DF}}$$

$$I_{\text{LC}}(t) = K_{\text{LC}} + \mathcal{N}_{\text{sn}}(t)_{\text{LC}}$$

and for the mean total intensity:

$$\bar{I} = I_{\text{bck}} + (K_{\text{DF}} + \lambda_{\text{DF}}S) + (K_{\text{LC}} + \lambda_{\text{LC}}S) \times (1 - c_1)$$

The power spectra of the signal described above, taking into account the finite duration T of the light curves and adopting the normalization of Leahy (1983) is:

$$P(\nu) = P_0 + P_{\text{RN}} + P_{\text{HL}} + P_{\text{CPL}} + P_{\text{WN}} \quad (1)$$

The first term is the power at zero frequency and is only dependent on the total intensity of the signal.

$$P_0 = N\bar{I}^2 T W_T^2(\nu) \quad (2)$$

where $N = 2/\bar{I}$ is the normalization constant according to Leahy and where $W_T^2(\nu) = \sin^2(\pi\nu T)/(\pi\nu T)^2$ is the window function. We note that $P_0 = 0 \forall \nu_k = k/T$ where the

Fourier frequencies are computed at $k = 1, \dots, (T/2\Delta t) - 1$. For this reason P_0 has not been included in the fit discussed in §3. The red noise (RN) term is

$$P_{\text{RN}} = N \times (\lambda_{\text{DF}} + (1 - c_1)^2 \lambda_{\text{LC}}) S^2 f_{\text{RN}}(\nu) \quad (3)$$

where, in the simplest case of a shot noise process obtained from the random superposition of identical shots, $f_{\text{RN}}(\nu) = |H(\nu)|^2 / \text{MAX}\{|H(\nu)|^2\}$, in a more general case $f_{\text{RN}}(\nu)$ is a non negative function normalized to 1 that describes the shape of the red noise. The harmonic line term is given by:

$$P_{\text{HL}} = N \times (c_1/2)^2 \times (K_{\text{LC}} + \lambda_{\text{LC}} S)^2 \times T W_T^2(\nu - \nu_0) \quad (4)$$

where, because of the almost sinusoidal shape of the SAX J1808.4-3658 pulse profile, we have taken into account only the fundamental frequency. The coupling term is:

$$P_{\text{CPL}} = N \times (c_1/2)^2 \times \lambda_{\text{LC}} S^2 f_{\text{RN}}(\nu - \nu_0) \quad (5)$$

It consists in a rescaled versions of the red noise placed at the harmonic frequencies, the scaling factor is $r = P_{\text{CPL}}/P_{\text{RN}} = \frac{1}{4} \left(\frac{c_1}{(1-c_1)} \right)^2 \left(1 + \frac{\lambda_{\text{DF}}}{(1-c_1)^2 \lambda_{\text{LC}}} \right)^{-1}$. The white noise component P_{WN} , induced by counting statistics, has, adopting the normalization of Leahy, an expected value of 2. The actual value is usually (slightly) less than 2 because of detector dead-time effects (*e. g.* van der Klis 1989), thus its value will be determined by the fit of the power spectra, as described in §3.

We define the coupling fraction $\eta = \lambda_{\text{LC}} / (\lambda_{\text{LC}} + \lambda_{\text{DF}})$ as the ratio of the arrival rates of the localized shots over the total shot rate. Furthermore we define the pulsed fraction $\mathcal{P}_f = (M(t)_{\text{MAX}} - M(t)_{\text{MIN}}) / M(t)_{\text{MAX}} = 2c_1$, where $M(t)_{\text{MAX}}$ and $M(t)_{\text{MIN}}$ are respectively the maximum and the minimum of the modulating function over one period. With these definitions $0 \leq \mathcal{P}_f \leq 1$ and we have $c_1 / (1 - c_1) = \mathcal{P}_f / (2 - \mathcal{P}_f)$. Moreover, as $M(t) \geq 0$ always, we have $1/2 \leq (1 - c_1) \leq 1$ and $1 \leq 1 / (1 - c_1)^2 \leq 4$. Therefore the following relation must hold:

$$\frac{4\sqrt{r}}{\left[1 + \left(\frac{1-\eta}{\eta} \right)^{-1/2} \right]^{-1/2} + 2\sqrt{r}} \leq \mathcal{P}_f \leq \frac{4\sqrt{r}}{\left[1 + 4 \left(\frac{1-\eta}{\eta} \right) \right]^{-1/2} + 2\sqrt{r}} \quad (6)$$

In the following section we will determine r from the fit of the power spectra and with relation (6) we will constrain the values of the pulsed fraction in relation to the fraction of coupled shots.

Moreover we will be able to derive a relation between the diffuse component of the signal, as defined above, and the pulsed fraction. Averaging the signal only over the shot noise process we define:

$$\langle I(t) \rangle = I_{\text{bck}} + (K_{\text{DF}} + \lambda_{\text{DF}} S) + (K_{\text{LC}} + \lambda_{\text{LC}} S) \times (C + c_1 \cos(2\pi \nu_0 t)) \quad (7)$$

thus

$$\begin{aligned}\langle I(t) \rangle_{\text{MAX}} &= I_{\text{bck}} + (K_{\text{DF}} + \lambda_{\text{DF}}S) + (K_{\text{LC}} + \lambda_{\text{LC}}S) \\ \langle I(t) \rangle_{\text{MIN}} &= I_{\text{bck}} + (K_{\text{DF}} + \lambda_{\text{DF}}S) + (K_{\text{LC}} + \lambda_{\text{LC}}S) \times (1 - 2c_1)\end{aligned}$$

We can therefore define the “observed” pulsed fraction

$$\mathcal{P}_{f \text{ obs}} = (\langle I(t) \rangle_{\text{MAX}} - \langle I(t) \rangle_{\text{MIN}}) / (\langle I(t) \rangle_{\text{MAX}} - I_{\text{bck}})$$

with a little algebra we can derive $\mathcal{P}_{f \text{ obs}} = 2c_1 / \left(\frac{K_{\text{DF}} + \lambda_{\text{DF}}S}{K_{\text{LC}} + \lambda_{\text{LC}}S} + 1 \right) = 2c_1 / \left(\frac{\langle I_{\text{DF}} \rangle}{\langle I_{\text{LC}} \rangle} + 1 \right)$. Recollecting that $\mathcal{P}_f = 2c_1$ we can derive $\frac{\langle I_{\text{DF}} \rangle}{\langle I_{\text{LC}} \rangle} = \frac{\mathcal{P}_f}{\mathcal{P}_{f \text{ obs}}} - 1$. We can now define the diffuse fraction as the ratio of the diffuse component over the sum of the diffuse and localized components as $\xi = \frac{\langle I_{\text{DF}} \rangle}{\langle I_{\text{DF}} \rangle + \langle I_{\text{LC}} \rangle}$. Using the relations above we have $\xi = 1 - \frac{\mathcal{P}_{f \text{ obs}}}{\mathcal{P}_f}$. We will see in the next section how the constraints on the pulsed fraction will have a bearing also on the fraction of the diffuse component.

3. Data analysis and results

We used the observations of SAX J1808.4-3658 performed by the Rossi X-Ray Timing Explorer (RXTE) during the April-May 1998 outburst (see Table 1). In particular we examined the data from the Proportional Counter Array (PCA) (Jahoda et al. 1996) which is composed of a set of five xenon proportional counters sensitive to X-rays in the 2 - 60 keV range with a total area of $\sim 7000 \text{ cm}^2$ and a 1° FWHM field of view. We used data collected with $\sim 122 \mu\text{s}$ time resolution and 64 PHA channels which were available for all observations (except for the April 13 observation which was excluded from our analysis).

We first corrected photons arrival times for satellite motion with respect to the solar system barycenter using the BeppoSax position for the source (in 't Zand et al. 1998) $R.A. = 18h08m29s$, $Dec = -36^\circ 58.6'(J2000)$. We then corrected for the orbital motion of the neutron star by using the orbital parameters derived by Chakrabarty & Morgan (1998). For our analysis we rebinned the data into bins of $\Delta t = 488.28125 \mu\text{s}$ (corresponding to a Nyquist frequency of 1024 Hz) and we used the events from all 64 PHA channels. The resulting lightcurves were used for the subsequent analysis.

For each observation, we calculated consecutive FFTs over time intervals of $T = 64\text{s}$ corresponding to power spectra with a frequency range of 0.015625-1024 Hz. These power spectra were then averaged to produce a single power spectra for each observation, 16 in all.

The source flux decreased across the observations by a factor of ~ 100 (Gilfanov et al. 1998). The aperiodic variability was determined to change with flux level (Wijnands

& van der Klis, 1998b). On the other hand, the simple model of the aperiodic variability described in the previous section assumes that the characteristics of the signal do not vary with time. Thus in our analysis we selected and analyzed only the observations in which the source count rate was highest (between ~ 800 and ~ 500 cts/s). In particular we selected the 6 consecutive observations between April 11 and 20. Examining the power spectra of each observation we consistently find an almost constant value for the red noise intensity and shape.

The shape of the red noise in SAX J1808.4-3658 was found to be reasonably well described by the sum of three empirical functions:

$$f_{\text{RN}}(\nu) = \sum_{i=1}^3 p_i f_i(\nu)$$

where: $f_i(\nu) = [1 + (2\pi\tau_i\nu)^{\alpha_i}]^{-1}$ and p_i indicates the normalization of each of them.

In order to fit the spectrum efficiently, we logarithmically rebinned the spectrum so that the number n_i of original bins averaged in the i^{th} new bin follows $n_i = \text{int}(1.02^i)$, where $\text{int}(x)$ is the integer part of x . The region around the coherent modulation peak ($400.8 < \nu < 401.2$) was left at the original Fourier resolution, while the intervals $352.37 < \nu \leq 400.8$ and $401.2 \leq \nu < 449.64$, in which the peak broadening would be more important, were (uniformly) rebinned by a factor of 31 (see Fig. 1). The region around the second harmonic of the modulation was excluded (see above). We used a fitting function :

$$F(\nu) = A_1 f(\nu) + A_2 g(\nu - \nu_0) + A_3 f(\nu - \nu_0) + A_4$$

where $g(\nu) = W_T^2(\nu)$ and $f(\nu) = p_1 f_1(\nu) + p_2 f_2(\nu) + p_3 f_3(\nu)$ as defined above. Thus $A_1 f(\nu) = P_{\text{RN}}$, $A_2 g(\nu - \nu_0) = P_{\text{HL}}$, $A_3 f(\nu - \nu_0) = P_{\text{CPL}}$ and $A_4 = P_{\text{WN}}$.

In order to check the robustness of our fit we compared different fitting procedures. a) In the first place we have tried a global fit, that is we simultaneously fit the whole range leaving all the parameters of the fit free to vary. Then, keeping fixed the parameters that describe the three empirical functions f_i , namely p_i , α_i , τ_i , we compare the fit on the whole range leaving A_1 , A_2 and A_3 free and leaving just A_1 and A_2 free and forcing $A_3 = 0$, that is imposing the hypothesis of null coupling. We obtain two values of the χ^2 with $\Delta\chi^2 = \chi_1^2 - \chi_2^2 = 19$. b) In second instance we repeated the procedure we compare the fit before and after freezing $A_3 = 0$ only in the region near the armonic line, between 396 and 406 Hz, the difference in the χ^2 we obtain is $\Delta\chi^2 = 21$. c) Last we wanted to check if the effect was still present freezing also A_2 , measuring the height of the harmonic line, thus we compared the fit in the same region of case b) and found that the $\Delta\chi^2 = 21$. We thus conclude that the region that affects the fit is only the narrow region around 401 Hz and a

significant coupling is present independently of the detailed fitting procedure. The values determined for case b) of the f_i and A_1, A_2, A_3 parameters are listed in Tab. 2 along with their errors. From the best fit parameters A_3 and A_1 we derive $r = P_{\text{CPL}}/P_{\text{RN}} = 0.005$. An F-test calculates the probability that the $\Delta\chi^2$ variation is due to a chance improvement $P = 8.38 \times 10^{-6}$.

With the derived value of r , we plot in figure (2) the two constraints defined by equation (6) in the $\eta - \mathcal{P}_f$ plane. The area between the curves defines the allowed region for the parameters. It can be seen that for any allowed value of the pulsed fraction a fraction of shots between 0.8 – 100% must be modulated at the spin period (coupled). Moreover, even in the most favourable case of 100% localized shots, the modulation has to be $> 17\%$ in order to account for the broadening detected. It can be noted that, in our discussion, we have assumed an identical amplitude for the localized and diffuse shots, that is, we have assumed that the blobs originating in the disk survive intact to the polar caps. It might be argued that the magnetic field just scoops off a fraction of each blob. We examined, for example, a case in which just 10% of each blob is threaded to the neutron star surface. In this scenario we obtain that nothing much changes in the favourable case of total coupling (100%), whilst for the maximum value of the pulsed fraction (100%), a minimum fraction of shots greater than 45% must be modulated at the spin period. That is, if just a part of each blob is scooped off, then more blobs must be funneled to observe the same effect.

A different constraint can be derived comparing the “observed” pulsed fraction value $\mathcal{P}_{f \text{ obs}}$ with its theoretical value \mathcal{P}_f as derived from eq. 6 above. To compute the value of the “observed” pulsed fraction we have folded the data corrected for the orbital motion modulo the spin period and obtained a pulse profile. Adopting the background value for this observation of 130 c/s (Wijnands & van der Klis 1998a) we found $\mathcal{P}_{f \text{ obs}} \sim 12\%$. We can note from fig. (2) that the pulsed fraction $0.17 \leq \mathcal{P}_f \leq 1$ and, recollecting the definition of the fraction of diffuse component $\xi = 1 - \frac{\mathcal{P}_{f \text{ obs}}}{\mathcal{P}_f}$ we can pose a constraint on ξ , $1 - \frac{\mathcal{P}_{f \text{ obs}}}{1} \leq \xi \leq 1 - \frac{\mathcal{P}_{f \text{ obs}}}{\mathcal{P}_{f \text{ min}}}$, and so $0.294 \leq \xi \leq 0.88$. We can now plot in fig (3) the diffuse fraction ξ , versus the fraction of coupled shots η .

4. Summary and Conclusions

We have shown the presence of a broadening at the base of the harmonic line. This can be interpreted as the result of a coupling between a fraction (between 0.8% and 100%) of the aperiodic and periodic variability in SAX J1808.4-3658. Moreover we have demonstrated that a fraction between $\sim 30\%$ and $\sim 90\%$ of the total emission arises from a component that is not modulated by the lighthouse effect (diffuse component).

Some more stringent constraints can be derived if we assume that the diffuse component originates from an accretion disk and the localized component derives from accretion onto the neutron star surface. As the spin period of SAX J1808.4-3658 is known, we can compute the corotation radius for this system *i.e.* the radius at which the speed of a particle rigidly rotating with the neutron star equals the local Keplerian value, $R_{\text{co}} = 1.5 \times 10^6 m^{1/3} P_{-3}^{2/3}$ cm, where m is the NS mass in units of solar masses and P_{-3} is the NS spin in milliseconds. In our case we get $R_{\text{co}} = 30.8$ km assuming a mass of $1.4M_{\odot}$. For the accretion not to be centrifugally inhibited the inner rim of the disc must be located inside the corotation radius. Therefore we have $R_{\text{disc}} \leq R_{\text{co}}$. In the standard scenario of disk accretion onto magnetized neutron stars, the accreting matter forms a disk whose inner radius is truncated at the magnetosphere by the interaction of the accretion flow with the magnetic field of the NS. In this case the magnetospheric radius r_{m} is a fraction $\phi \lesssim 1$ (an expression for ϕ can be found in Burderi et al. 1998¹; for $L \sim 10^{36}$ ergs/s we get $\phi \sim 0.3$) of the Alfvén radius R_{A} defined as the radius at which the energy density of the (assumed dipolar) NS magnetic field equals the kinetic energy density of the spherically accreting (free falling) matter:

$$R_{\text{A}} = 2.23 \times 10^6 R_6^{-2/7} m^{1/7} \mu_{26}^{4/7} \epsilon^{2/7} L_{37}^{-2/7} \text{ cm} \quad (8)$$

(see, e.g., Hayakawa 1985), where R_6 is the NS radius, R_{NS} , in units of 10^6 cm, m is the NS mass in solar masses, μ_{26} is the NS magnetic moment in units of 10^{26} G cm³, ϵ is the ratio between the specific luminosity and the specific binding energy ($L = \epsilon \times GMM/\dot{R}_{\text{NS}}$, G is the gravitational constant, M is the NS mass, \dot{M} is the accretion rate), and L_{37} is the accretion luminosity in units of 10^{37} erg/s, respectively. In this context we have $R_{\text{disc}} = r_{\text{m}}$. Since the accretion disc is virialized, its luminosity (averaged over the shot process) is $\langle I_{\text{DF}} \rangle = 0.5 \epsilon G M \dot{M} / r_{\text{m}}$. The total luminosity is $\langle I_{\text{DF}} \rangle + \langle I_{\text{LC}} \rangle = \epsilon G M \dot{M} / R_{\text{NS}}$. Therefore we have $\xi = 0.5 R_{\text{NS}} / r_{\text{m}}$. A lower limit for the inner rim of the accretion disk is $r_{\text{m}} \geq R_{\text{NS}}$ and therefore we get the constraint $\xi \leq 0.5$. This constraint is indicated as a dashed horizontal line in fig. 3. This immediately gives a lower limit on the fraction of coupled shots $\eta > 42\%$ indicated ad the dashed vertical line in figures 2 and 3. This in turn limits the value of the pulsed fraction below 0.37 as indicated in fig. 2 by the dashed horizontal line. An upper limit can be derived from the constraint derived in the previous paragraph $\xi \geq 0.294$ that gives $r_{\text{m}} \leq 1.7 R_{\text{NS}}$. Adopting as a typical NS radius $R_{\text{NS}} \sim 10$ km, we get $r_{\text{m}} \leq 17$ km, that is consistent with the requirement that accretion is not centrifugally inhibited. Moreover adopting $\phi = 0.3$ we can derive an upper limit for the magnetic field of the NS. Adopting the explicit espression for Alfvén radius in $r_{\text{m}} \leq 1.7 R_{\text{NS}}$ we obtain $\mu_{26} \leq 5.1 \phi_{0.3}^{-7/4} R_6^{9/4} m^{-1/4} \epsilon^{-1/2} L_{37}^{1/2}$, where $\phi_{0.3}$ is the ϕ factor in units of 0.3. Taking

¹ $\phi = 0.21 \alpha^{4/15} n_{0.615}^{8/27} m^{-142/945} [(L_{37}/\epsilon)^{8/7} R_6^{8/7} \mu_{26}^{5/7}]^{4/135}$, see the text for the definition of the symbols.

$m = 1.4$, $\epsilon = 1$ and $L_{37} = 0.1$ that are appropriate for our source, we get $\mu_{26} \leq 1.5 R_6^{9/4}$. This is well within the range $(1 - 5) \times 10^{26}$ G cm³ that are the lower and upper limits derived by Chakrabarty (199) and di Salvo & Burderi (2002) respectively.

This scenario implies that the aperiodic variability is generated in a region affected by the lighthouse modulation, close to the neutron star surface. Our result is in line with the coupling of the red noise discovered analyzing the power spectra of some high mass X-ray binaries (B97, LS97). Our present result constrains some of the models proposed for the origin of the aperiodic variability. Indeed a scenario like the one proposed by Aly & Kuijpers (1990) in which the aperiodic variability is generated by a shot noise process associated with magnetospheric flares, caused by magnetic reconnection all around the neutron star magnetosphere, cannot work for the origin of the aperiodic variability in SAX J1808.4-3658 in case the red noise component were coupled with the periodic modulation. On the other hand, inhomogeneities could arise in the accretion flow during the plasma penetration in the magnetosphere (*e.g.* via Kelvin-Helmholtz instabilities, see B97 for a more extensive discussion). The subsequent impact of this inhomogeneous accretion flow funneled by the magnetic field lines onto the magnetic caps appears to be a viable mechanism for the origin of the red noise.

This work was partially supported by a grant from the Italian Ministry of University and Research (Cofin 2001021123_002). We warmly thank the referee for very useful and stimulating criticism.

REFERENCES

- Aly, J. J. & Kuijpers J. 1990, A&A, 227, 473
- Belloni, T., Hasinger, G., 1990, A&A, 230, 103
- Burderi, L., Robba N. R., Cusumano, G. 1993, Adv.SpaceRes., 13(12), 291
- Burderi, L., Robba, N. R., La Barbera, N., Guainazzi, M. 1997, ApJ, 481, 943 (B97)
- Burderi, L., di Salvo, T., Robba, N. R., del Sordo, S., Santangelo, A., Segreto, A. 1998, ApJ, 498, 831
- Chakrabarty, D., Morgan, E. H. 1998, Nature, 394, 346-348
- di Salvo, T., Burderi, L. 2002, A&A, 397, 723

- Gilfanov, M. et al. 1998, *A&A*, 338, L83-L86
- Hayakawa, S. 1985, *Phys. Rep.*, 121, 317
- Heindl, W.A. & Smith, D.M. 1998, *ApJ*, 506, L35-L38
- in 't Zand, J.J. et al. 1998, *A&A*, 331, L25-L28
- in 't Zand, J.J. et al. 2001, *A&A*, 372, 916
- Jahoda, K., Swank, J.H., Giles, A.B., Stark, M.J., Strohmayer, Tod., Zhang, W., Morgan, E.H., 1996, *Proc. SPIE*, 2808, 59
- Lazzati, D., Stella, L. 1997, *ApJ*, 476, 267 (LS97)
- Lehay, D. A., et al. 1983, *ApJ*, 266,160
- Moon, D., Eikenberry, S.S. 2001, *ApJ*, 552, L135-139
- van der Klis, M. 1989, in *Fourier Techniques in X-ray Timing, Timing Neutron Stars*, ed. H. Ogelman, & E. van den Heuvel (Kluwer Academic Publishers, Dordrecht), 27
- Wijnands, R., van der Klis, M. 1998a, *Nature*, 394, 344
- Wijnands, R., van der Klis, M. 1998b, *ApJ*, 507, L63-L66
- Wijnands, R., van der Klis, M. 1999, *ApJ*, 514, 939

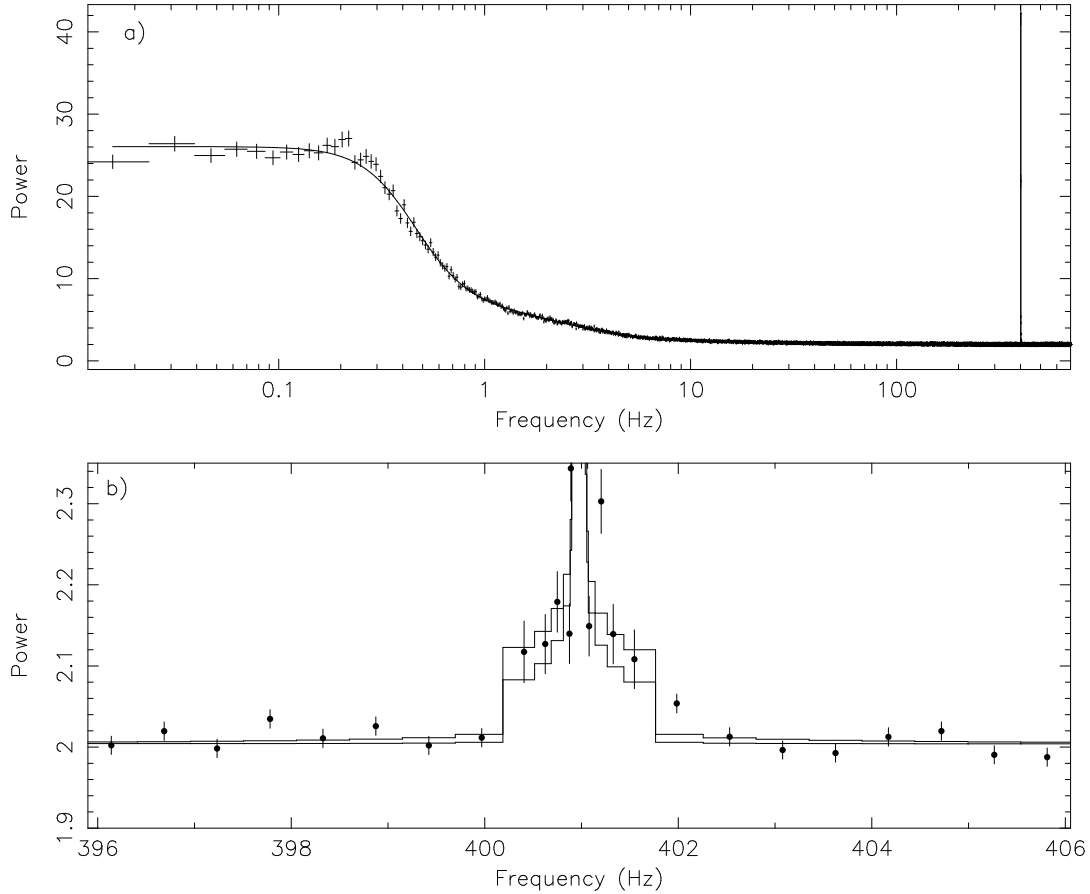


Fig. 1.— The power spectrum of SAX J1808.4-3658. Upper panel shows the measured broad band power spectrum and the simultaneous modelling of the red noise and harmonic components (solid line). The lower panel shows an expanded view of the region around the first fundamental harmonic: data have been binned by a factor 35 to increase the signal to noise ratio. Both the fit with and without coupling with the red noise have been plotted. The lower line is without coupling. (Note that in the case of no coupling the residual broadening at the base of the harmonic line is due to the convolution of the delta function representing periodic modulation with the Fourier transform of the box function of duration T that multiplies the signal because of the finite duration of the observation).

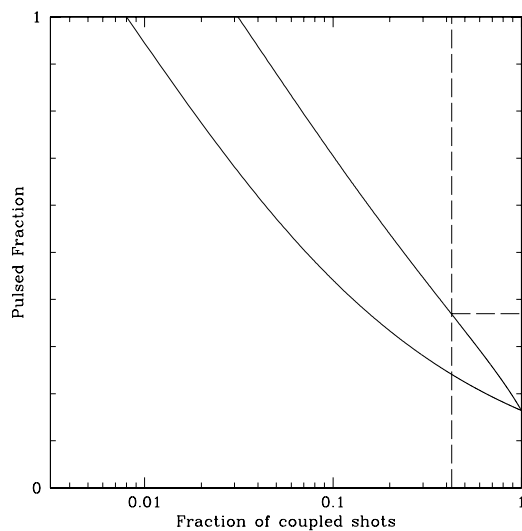


Fig. 2.— The \mathcal{P}_f vs η relation. The dashed vertical line indicates a lower limit on the fraction of coupled shots $\eta \geq 0.42$ derived from the constraints of Fig. 3. This, in turn, poses an upper limit on the pulsed fraction $\mathcal{P}_f \leq 0.37$.

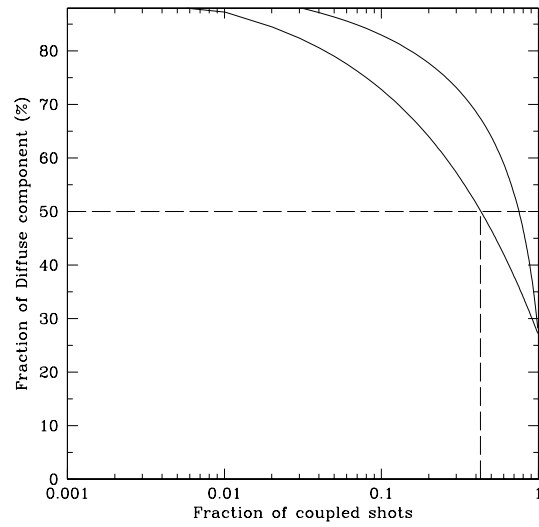


Fig. 3.— The ξ vs η relation. The horizontal line indicates an upper limit for the fraction of diffuse component $\xi \leq 50\%$. This, in turn, poses a lower limit on the fraction of coupled shots $\eta \geq 0.42$, as shown by the dashed vertical line.

Table 1: Observations log

Observation ID	Start Time	End Time	used in this work
30411-01-01-00	11-4-1998 19:13	11-4-1998 21:56	n
30411-01-02-00	13-4-1998 01:23	13-4-1998 02:22	n
30411-01-03-00	16-4-1998 17:02	16-4-1998 22:59	y
30411-01-04-00	17-4-1998 01:11	17-4-1998 04:40	y
30411-01-05-00	18-4-1998 02:54	18-4-1998 09:17	y
30411-01-06-01	18-4-1998 12:27	18-4-1998 13:32	y
30411-01-06-00	18-4-1998 14:04	19-4-1998 01:02	y
30411-01-07-00	20-4-1998 20:52	20-4-1998 23:07	y
30411-01-08-00	23-4-1998 15:47	23-4-1998 23:19	n
30411-01-09-01	24-4-1998 15:51	24-4-1998 17:14	n
30411-01-09-02	24-4-1998 17:28	24-4-1998 23:21	n
30411-01-09-03	25-4-1998 14:17	25-4-1998 15:28	n
30411-01-09-04	25-4-1998 15:49	25-4-1998 21:40	n
30411-01-09-00	26-4-1998 15:55	26-4-1998 23:26	n
30411-01-10-02	27-4-1998 14:19	27-4-1998 15:41	n
30411-01-10-01	27-4-1998 15:57	27-4-1998 19:29	n
30411-01-10-00	29-4-1998 14:08	29-4-1998 18:56	n
30411-01-11-02	2-5-1998 01:14	2-5-1998 02:57	n
30411-01-10-03	2-5-1998 03:37	2-5-1998 04:38	n
30411-01-11-00	3-5-1998 18:59	3-5-1998 21:00	n
30411-01-11-01	6-5-1998 10:52	6-5-1998 14:00	n

Table 2: Results of the fit

	Parameter	Value	Error (90% confidence level)
<i>WN</i>		1.994	± 0.001
<i>RN</i>	A_1	$1.7 \times$	$\pm 6 \times 10^{-1}$
	p_1	1.1×10^1	$\pm 0.6 \times 10^1$
	p_2	2.6	± 1
	p_3	1.6×10^{-1}	$\pm_9^8 \times 10^{-2}$
	τ_1	3.45×10^{-1}	$\pm_5^4 \times 10^{-3}$
	α_1	3.3	$\pm_2^3 \times 10^{-1}$
	τ_2	6.5×10^{-2}	$\pm_{0.5}^1 \times 10^{-2}$
	α_2	2.0	± 0.2
	τ_3	3.9×10^{-3}	$\pm 1. \times 10^{-3}$
	α_3	1.5	± 0.1
	A_2	7.3×10^1	± 3
	A_3	3.4×10^{-3}	$\pm 1 \times 10^{-3}$
Coupling	r	0.002	± 0.001